Accepted Manuscript

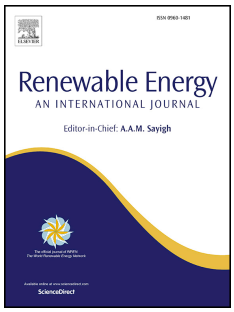

Motion and performance of BBDB OWC wave energy converters: I, hydrodynamics

Wanan Sheng

PII: S0960-1481(19)30016-3

DOI: https://doi.org/10.1016/j.renene.2019.01.016

Reference: RENE 11017

To appear in: *Renewable Energy*

Received Date: 26 February 2018

Revised Date: 23 December 2018

Accepted Date: 3 January 2019

Please cite this article as: Sheng W, Motion and performance of BBDB OWC wave energy converters: I, hydrodynamics, *Renewable Energy* (2019), doi: https://doi.org/10.1016/j.renene.2019.01.016.

Motion and performance of BBDB OWC wave energy converters: I, Hydrodynamics

Wanan Sheng

Centre for Marine and Renewable Energy Ireland (MaREI), Environmental Research Institute, University College Cork, Ireland. Email: w.sheng@ucc.ie

Motion and performance of BBDB OWC wave energy converters: Hydrodynamics

Wanan Sheng

SW Mare Maine Technology

Email: wanan_sheng@outlook.com

ABSTRACT

The Backward Bent Duct Buoy (BBDB) oscillating water column (OWC) wave energy converter (WEC) has been invented following the so-far most successful OWC navigation buoys in wave energy utilisation, with aims to build large and efficient OWC wave energy converters for massive wave energy production. The BBDB device could use its multiple motion modes to enhance wave energy conversion, however, the mechanism of the motion coupling and their contributions to wave energy conversion have not been well understood in a systematic manner. In particular, the numerical modelling has been very limited in exploring how these motions are coupled and how the wave energy conversion capacity can be improved.

As in this part of the research of a systematic study using numerical modelling, focus is on the understanding of the hydrodynamic performance for the BBDB OWC wave energy converter. In the study, the boundary element method based on potential flow theory has been applied to calculate the basic hydrodynamic parameters for the floating BBDB OWC structure and the water body in the water column in the BBDB OWC device. With the calculated hydrodynamic parameters and the decoupled and coupled models for the BBDB OWC dynamics, it is possible to examine these hydrodynamic parameters in details and to understand how they interact each other and how they contribute to the relative internal water surface motion, a most important response in terms of wave energy conversion of the OWC devices. All these will provide a solid base for further studying the power performance of the BBDB devices for converting energy from waves as shown in the second part of the research.

Keywords: Wave energy converter; oscillating water column; backward bent duct buoy (BBDB); frequency-domain analysis; hydrodynamic performance; wave energy conversion

1 INTRODUCTION

Wave energy is well known to have a potential to contribute to the renewable energy mix in future and remains one of the largest untapped renewable resources so far since the technologies are not matured enough for efficiently, reliably and economically extracting energy from sea waves [1, 2]. Researchers and developers have made great efforts in advancing wave energy technologies since 1799 when a French father and son filed a patent for their wave energy device and more than a thousand of wave energy technologies have been patented (see [3]). To date, the most successful story for wave energy utilisation would be the navigation buoys powered by wave energy, which were invented and developed by a Japanese, Yoshio Masuda, since 1940s, a pioneer in modern wave energy technologies. The developed navigation buoys were very successful: 700 buoys have been used in Japan, while other 500 have been sold to the other countries including 20 in the United States [4]. Based on the current terminology of wave energy technologies, those navigation buoys are in fact the oscillating water columns (OWCs). Interestingly, the OWC wave energy converters were first called the Masuda devices following the inventor's name, and much later named as oscillating water column as we used formally now, according to Ross [5]. Though it is not very clear when the name is firstly used, the references the author searched show that Evans used it in 1978 when he first formulated the relevant mathematical equations for the hydrodynamics of OWCs [6]. Though very successful in those OWC navigation buoys, Masuda had further worked on the OWC energy conversion principle, aiming to build large and efficient OWC wave energy converters for massive wave energy production, that is, first 'Kaimei' [7] and then Backward Bent Duct Buoy (BBDB) [4]. As a unique advantage for the OWC devices as pointed out by Evans [8], they may be the only wave energy converters which can effectively overcome the challenges for converting the low-frequency motion in waves (~0.1 Hz) into electricity of 50 or 60 Hz.

OWC wave energy converters are now being regarded as one of the most promising wave energy converters, and probably the most practical and reliable wave energy converters due to their inherent wave energy conversion principle. It is interesting to see that the most recent European Wave and Tidal Energy Conference (EWTEC 2017) (Cork, Ireland) (http://www.ewtec.org/ewtec-2017/) has shown a significantly increased interest in OWC wave energy technologies. While many other wave energy converters utilise the low-speed motion of the device structure(s) or water body (thus large forces) for direct power conversion, OWC wave energy converters employ the air flow driven by the internal water surface (IWS) motion (the relative motion between the structure and the water body in the water column) in the water column of the OWC devices. In the OWC power conversion from pneumatic power to mechanical power, the air flow driven by the IWS motion is normally accelerated by many times (roughly at 50-150 times [9]), and the accelerated air flow could drive the air turbine Power Take-offs (PTOs) in

high rotational speeds (up to 3000 rpm for the Wells turbines and 1500 rpm for impulse turbines [10]). This high rotational speed of the PTO system allows a low torque acting on the PTOs when compare to the direct conversion in many other wave energy technologies, and thus it is very beneficial for a high reliability in the OWC PTO and the other relevant components (including the structure of the device) in terms of a long-term wave energy production. This energy conversion principle is very analogous to the conventional power stations, where the steam turbines have a very high rotational speed, normally at 3000rpm or 3600 rpm (50Hz or 60Hz), hence allowing small torques acting the steam turbines, allowing a very high reliability in long-term energy production.

Currently, some OWC technologies have been progressed to high level of technology readiness levels, and a few of them even to practical wave energy plants/devices. The shoreline plants include LIMPET [11, 12], PICO [13, 14], Mutriku [15, 16] and the floating OWC devices includes the BBDB OE Buoy [17, 18]. It has been reported that the LIMPET OWC plant has generated electricity to the grid for more than 60,000 hours in a period of about 10 years [19], whilst OceanEnergy Ltd have sea-trialled their 1/4 scaled 'Back Bent Duct Buoy (BBDB)' in Galway Bay (Ireland) for more than 3 years [18]. At the time of writing this article, OceanEnergy Ltd are in the process of manufacturing a full scale OE buoy and are planning to undergo an open-sea trial in the open sea in Hawaii, US, in near future. In addition, a recent research report by the EU Joint Research Centre (JRC) [2] has shown that the current capacity factors achieved 25 % in the case of OWC wave energy converters and 10 % for other device types (capacity factor is defined as the ratio of the actual annual output of energy production divided by the rated power of the device and the hours of the year). Also in [2], the capacity factor for the economically viable ocean energy production is recommended at 30% - 40%. In this regard, OWC wave energy converters may be the wave energy technology which has a very close capacity factor level to the requirement.

To assess and optimise the hydrodynamic and power performance of the OWC devices, numerical methods and experimental methods both are important and have been used widely. Since Evans firstly formulated the theory for OWC devices in 1978 [6], numerical methods have been advanced a great deal, and both analytical and numerical models have been proposed and used [6, 9, 20-24]. Currently, two distinguishing methods in mathematical/numerical modelling are used for studying the OWC performance. The first approach is called the massless piston model [6, 25] for which the internal water surface (IWS) in the water column is taken as a massless rigid piston (a zero-thickness structure), and the motion of the internal water surface is solved together with other hydrodynamic parameters. A slightly different version of the massless piston model is a two-body system for the OWCs [9, 24, 26], in which the first rigid body is the device itself whilst the second rigid body is an imaginary piston (with a length) for replacing the internal water surface in the water column. In the latter method, when a PTO is applied

and coupled into the dynamic system, the pressure and the thus modified internal water surface in the air chamber can be solved using the coupling of the hydrodynamics and thermodynamics for the OWC devices (see [27]).

The second approach is the pressure distribution model [21], in which on the internal water-surface the dynamic air pressure is distributed [22, 28, 29]. In the numerical modelling, a reciprocity relation must be employed as shown by Falnes [30] such that the conventional boundary element methods (BEMs) can be used accordingly.

In linear cases, the two methods mentioned above can be only different when the higher-order motions in the water column are considered, and it is believed that the pressure distribution method is more suitable for accommodating the high-order motions in the water column [29]. However, for the purpose wave energy conversion, the heave motions account only. The higher-order motions do not contribute to the net wave energy conversion, and thus can be excluded in the analysis as it does in this research. A point should be noted here that in the OWCs with nonlinear air turbine PTOs, the numerical and experimental data have both shown that the pressures in the air chamber in OWC devices are much more nonlinear than that of the IWS motions. In this regard, solving the IWS motion first in the hydrodynamic module is more reasonable since the frequency-domain potential flow theory can not handle the nonlinear motions and forces.

As one type in the floating OWCs, the backward bent duct buoy (BBDB) OWC attracted a lot of interest from both researchers and developers since it was first shown by Masuda in 1987 [4]. Due to its unique design, the BBDB OWC devices could use its multiple motion modes to enhance the device power performance. This implies a more complicated hydrodynamic couplings among the motions and has made the numerical studies more difficult. As a result of such difficulties, the BBDB hydrodynamic and power performance are found to be difficult to be optimised because the strong interactions among the multiple motion modes, namely, surge, heave and pitch motions of the structure, as well as the internal water motion. This is why limited attempts have been made using numerical models for the BBDB converters [28, 31-33], and a systematic study on the hydrodynamics and thus the optimisations on the BBDB OWC devices have not been carried out effectively.

To streamline the development and provide the reference wave energy converters, National Renewable Energy Laboratory (NREL) and Sandia National Laboratory under the US DoE financial support have established the reference models for marine renewable energy (wave and tidal energy [34]). A BBDB has been chosen as one of three reference wave energy converters, named RM6 [23] (other two are: floating point absorber, RM3 and the bottom-fixed oscillating surging wave energy converter, RM5, see [35]). In

this research, a systematic study on the reference BBDB OWC is aimed to provide better understanding to its hydrodynamic and power performance.

In this research, focus is on the hydrodynamics of the RM6 BBDB, including some basic issues with the numerical convergence, coupling and decoupling of the motions and most importantly, how to identify and how to optimise the device so that an improved device would have better motion performance for more efficient wave energy conversion. The work is arranged as follows: in Section 2, the RM6 model is briefly introduced, together with a short description of panels used for the numerical modelling; Section 3 gives the introduction to the methodologies used in this study; in Section 4, a validation is made using the available published data, while Section 5 gives the approaches for improving hydrodynamic and power performance. The conclusions are drawn in Section 6.

2 RM6 REFERENCE MODEL

Reference Model 6 (RM6) is a Backward Bent Duct Buoy (BBDB) oscillating water column wave energy converter, which was designed as part of the DOE sponsored Reference Model Project [35] (see Figure 1). The BBDB has a horizontal water column of 35m long, 14m high and 27m wide and a vertical water column of an area of 17.5m*27m (472.5m^2).

To study the BBDB OWC device, the panels/patches used in numerical modelling can be seen in Figure 2. The coordinate origin for studying the motions and forces on this particular OWC device is located at the centre of the free surface in the water column (see Figure 2), with x-y plane on the calm water surface, and z-axis pointing up. This approach could simplify the motion and the force analysis and avoid the manipulations of the motion and force transformation (from the centre of gravity to the centre of free surface in the water column). In the chosen coordinate, the translational motions (named the motions along x-axis, y-axis and z-axis, respectively) will be different from those at the centre of gravity (named formally surge, sway and heave). However, for a purpose of simplification, the translational motions at the chosen coordinate will be still called as surge, sway and heave in the following analysis.

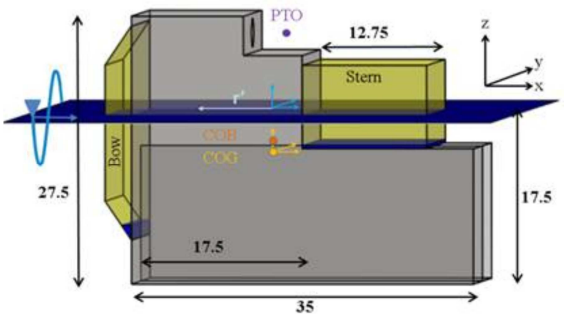

148 *Figure 1 RM6 design model (from [23])*

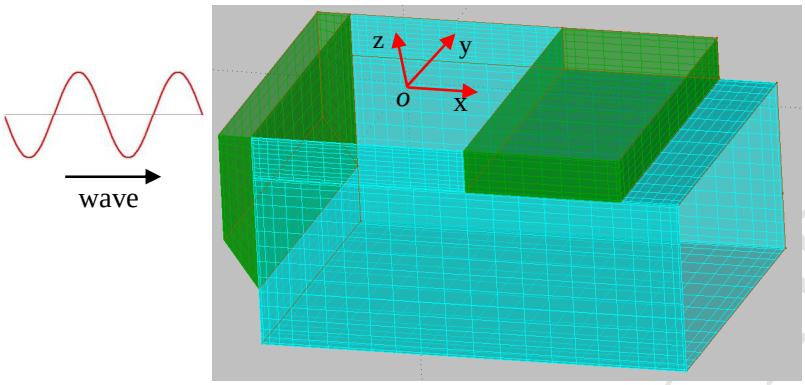

149

150 *Figure 2 Panels on RM6 for hydrodynamic analysis (green: solid surfaces, Cyan: panels for thin structures)*

151 The matrix for inertia is defined by following the WAMIT manual [36],

$$M = \begin{bmatrix} m & 0 & 0 & 0 & mz_g & -my_g \\ 0 & m & 0 & -mz_g & 0 & mx_g \\ 0 & 0 & m & my_g & -mx_g & 0 \\ 0 & -mz_g & my_g & I_{11} & I_{12} & I_{13} \\ mz_g & 0 & -mx_g & I_{21} & I_{22} & I_{23} \\ -my_g & mx_g & 0 & I_{31} & I_{32} & I_{33} \end{bmatrix} \quad (1)$$

152 where m is the mass, (x_g, y_g, z_g) are the coordinates of the centre of gravity in the body coordinate system.

153 The moments of inertia are defined are given in Newman's book ([37], p307), as

$$\begin{cases} I_{11} = \iiint_V \left(y^2 + z^2\right) dm_0 \\ I_{22} = \iiint_V \left(x^2 + z^2\right) dm_0 \\ I_{33} = \iiint_V \left(x^2 + y^2\right) dm_0 \\ I_{12} = I_{21} = -\iiint_V xy dm_0 \\ I_{13} = I_{31} = -\iiint_V xz dm_0 \\ I_{23} = I_{32} = -\iiint_V yz dm_0 \end{cases} \quad (2)$$

154 where V represents the whole volume of the structure, and dm_0 the distributed mass of the structure.

155 Based on the structure as above, the device has a displacement of 1995.84 m^3, and the radii of moments of
156 inertia at the centre of gravity are given in Table 1.

157 Table 1 Radii of the moment of inertia (taken from [23])

R_{xx} =12.53m	R_{xy} =0m	R_{xz} =3.35m

R_{yx} =0m	R_{yy} =14.33m	R_{yz} =0m
R_{zx} =3.35m	R_{zy} =0m	R_{zz} =14.54m

3 METHODOLOGIES

In this research, the two-body system is used, with the structure of the BBDB device being taken as the first body and the piston for replacing the water body in the water column as the second body. The motions and forces will be calculated based on the chosen coordinate (see above), with the centre of gravity of the structure at (5.16m, 0, -4.29m) [23].

3.1 Two-body system

Considering the BBDB wave energy converter, it may experience 6 DOF motions in waves. In the body coordinate, only the heave motions of the structure and the piston, more specifically, their relative motion contributes for pneumatic power conversion. However, since the complicated structure, both heave motions may be strongly coupled with other motion modes. Hence for a completion, following motion modes must be included in the dynamic equation, with 6-DOF motions for the structure and one motion mode for the piston. The other motion modes for the piston are ignored because the piston can be taken as a very thin structure, hence they could not contribute to the dynamic system. For this reason, the heave motion of the piston is re-defined as motion mode No. 7 for a convenience in the following analysis):

X_1: surge motion of the structure;

X_2: sway motion of the structure;

X_3: heave motion of the structure;

X_4: roll motion of the structure;

X_5: pitch motion of the structure;

X_6: yaw motion of the structure;

X_7: heave motion of the 'imaginary piston'.

In the frequency domain, the dynamic equation for the RM6 BBDB OWC with an air turbine PTO in waves can expressed as

$$\begin{pmatrix} a_{11} & a_{12} & a_{13} & a_{14} & a_{15} & a_{16} & a_{17} \\ a_{21} & a_{22} & a_{23} & a_{24} & a_{25} & a_{26} & a_{27} \\ a_{31} & a_{32} & a_{33} & a_{34} & a_{35} & a_{36} & a_{37} \\ a_{41} & a_{42} & a_{43} & a_{44} & a_{45} & a_{46} & a_{47} \\ a_{51} & a_{52} & a_{53} & a_{54} & a_{55} & a_{56} & a_{57} \\ a_{61} & a_{62} & a_{63} & a_{64} & a_{65} & a_{66} & a_{67} \\ a_{71} & a_{72} & a_{73} & a_{74} & a_{75} & a_{76} & a_{77} \end{pmatrix} \begin{pmatrix} X_1 \\ X_2 \\ X_3 \\ X_4 \\ X_5 \\ X_6 \\ X_7 \end{pmatrix} = \begin{pmatrix} F_1 \\ F_2 \\ F_3 + pA_0 \\ F_4 \\ F_5 \\ F_6 \\ F_7 - pA_0 \end{pmatrix} \tag{3}$$

with

$$a_{jk} = -\omega^2 \left(M_{jk}\delta_{jk} + A_{jk} \right) + i\omega \left(B_{jk} + B_{jk}^{vis} \right) + C_{jk} \quad (j, k=1,\ldots,7) \tag{4}$$

where δ_{jk} =1 when j =k and δ_{jk} =0 ($j \neq k$); M_{jj}=M_j is the corresponding mass or moment of inertia of the bodies based on the motion modes as defined as above; A_{jk}, B_{jk} and C_{jk} are the added mass, radiated damping coefficients and the restoring coefficients; B_{jk}^{vis} is the linear viscous damping coefficient; X_j the complex motion amplitude of the corresponding motion mode; F_j the complex excitation; p the complex chamber gauge pressure (note: the positive pressure in the air chamber will increase the heave motion of the structure, and reduce the heave motion of the piston. In the case without a PTO, the chamber pressure p=0); and A_0 the sectional area of the water column at water plane.

3.2 Numerical convergence

In this numerical modelling, the higher-order panel method is used in the BEM analysis (see [36]). By controlling the relevant parameters in the numerical modelling, the number of unknowns in linear dynamic system can be different for studying the numerical convergence. In the comparisons, the unknowns solved in the linear system are 1788 for the fine panels and 1258 for the coarse panels, respectively. For these two quite different panels, the RAOs of the motions are almost identical, with some very small differences at the peaks. This confirms that the convergence of the numerical modelling has been well achieved and gives the confidence to obtain the relevant hydrodynamic parameters for further analyses.

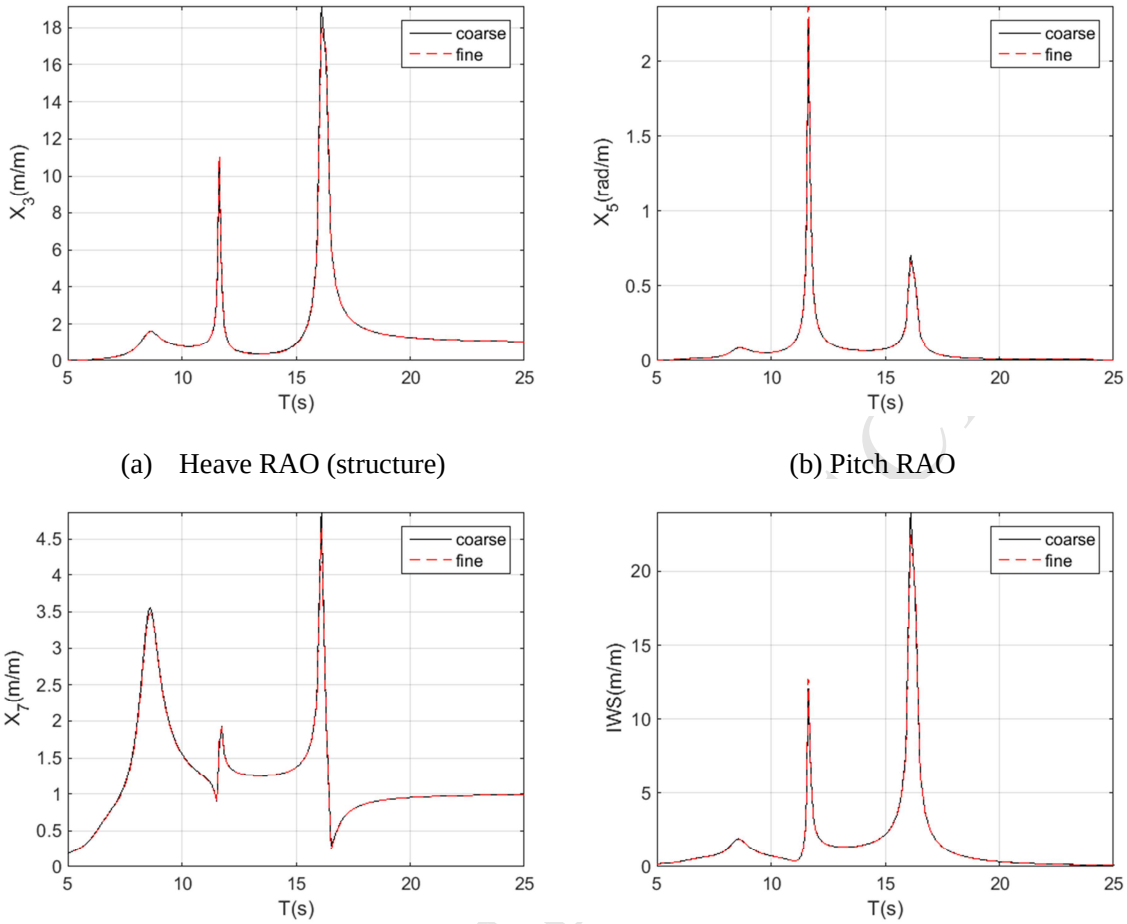

(a) Heave RAO (structure) (b) Pitch RAO

(c) Heave RAO ('piston') (d) Relative motion RAO

Figure 3 RAO comparisons for cases of different panels

3.3 Linear viscous damping

In the boundary element method, only the damping from the radiated wave is included. In reality, other types of damping may exist, for instance, damping from the viscosity of the water. In this study, a linear viscous damping is adopted by following Bull [28], with a form as

$$B_{jj}^{vis} = 0.04\sqrt{(m_{jj} + A_{jj})C_{jj}} \quad (j = 1,\ldots,7) \tag{5}$$

This is a generic linear viscous damping coefficient expression, usable for general purposes. However, for specific wave energy converters, the linear viscous damping coefficients may be needed to be adjusted for a better representation of the effect of viscous damping, depending on the practical design of the wave energy converters.

The choice of the additional linear damping is for two reasons: the first reason is that the additional linear damping could allow the frequency domain analyses, which could simplify the dynamic problem significantly; and the second reason is that the application of the additional linear damping could limit the motion responses within an acceptable range as those nonlinear additional damping coefficients, although these linear additional damping coefficients may be only applicable for a certain limited motion amplitude.

With the added linear viscous damping ('with viscous damping' in the figures), the RAOs are much more acceptable when compared to the RAOs without viscous damping ('no viscous damping'). The RAOs of heaves (structure and piston), piston and the internal water surface ('IWS' in the figure) with the given additional damping shown in Eqs. (5) and the RAOs without additional damping coefficients are compared in Figure 4. It can be seen that with the additional damping coefficients, the maximal RAOs of the heave and IWS motions are more acceptable. For instance, the maximal heave RAO is about or less than 2 both for the structure and for the piston, and the relative motion of the water body in the water column is less 3.

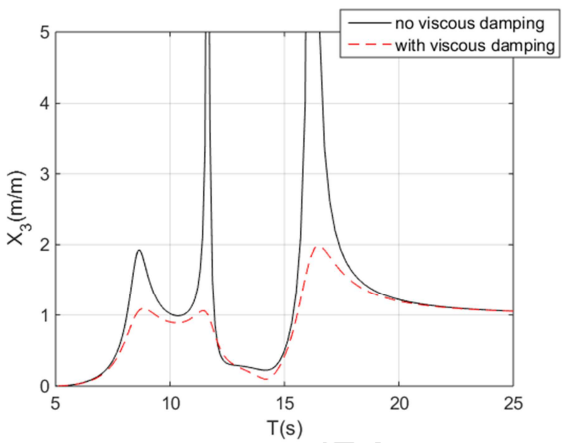

(a) Heave RAOs (structure)

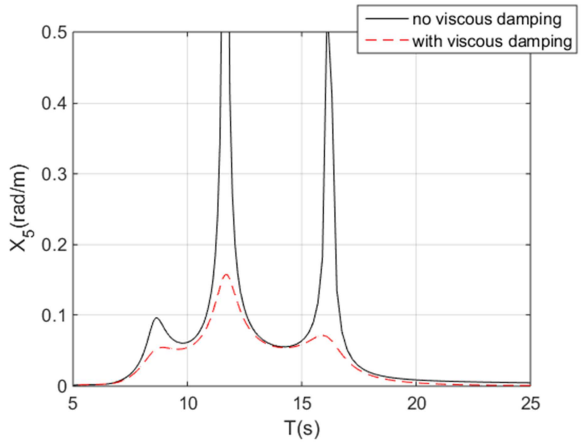

(b) Piston RAOs (structure)

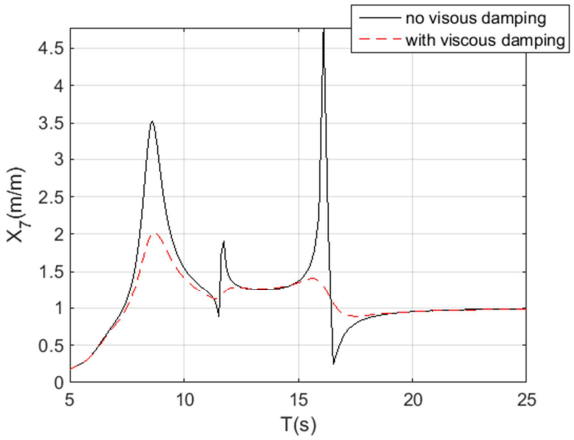

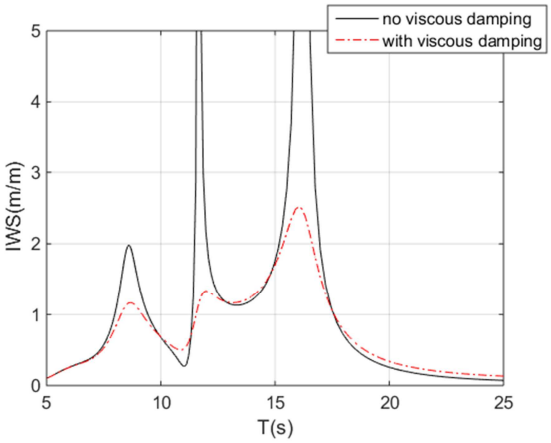

(c) Heave RAOs (piston) (d) Relative RAOs

Figure 4 RAOs of motions with and without linear viscous damping

3.4 Added mass and damping coefficients (radiated)

To examine the couplings between the motion modes in the RM6 BBDB OWC wave energy converter, its added mass and damping coefficients for both self- and cross- terms have been studied in an incident angle 45° of the waves, such a wave direction that all couplings between motion modes can be easily sorted out.

3.4.1 Self-radiated added mass and damping coefficients

The self-radiated added mass and damping coefficients are important in the dynamic system, and generally they are frequency-dependent. Figure 5 shows all these curves: added mass and damping coefficients are both similar in shapes (Figure 5a and Figure 5b for added mass and damping coefficients respectively), but the magnitudes of the RAOs can be very different. For instance, the added moment of inertia and the damping coefficient for pitch have much larger values (in the figures their values are reduced by 100 times for better comparisons). The added masses have the most frequency-dependent values in the short wave periods from 2-10s, but asymptote to constants at large waver periods. The damping coefficients have normally maximal values between 7-8s, and asymptote to zero at both zero wave period and frequency. Obviously, the maximal damping coefficients are be very different for different motion modes.

From Figure 5, it can be seen that all the self-radiated added masses and damping coefficients are positive.

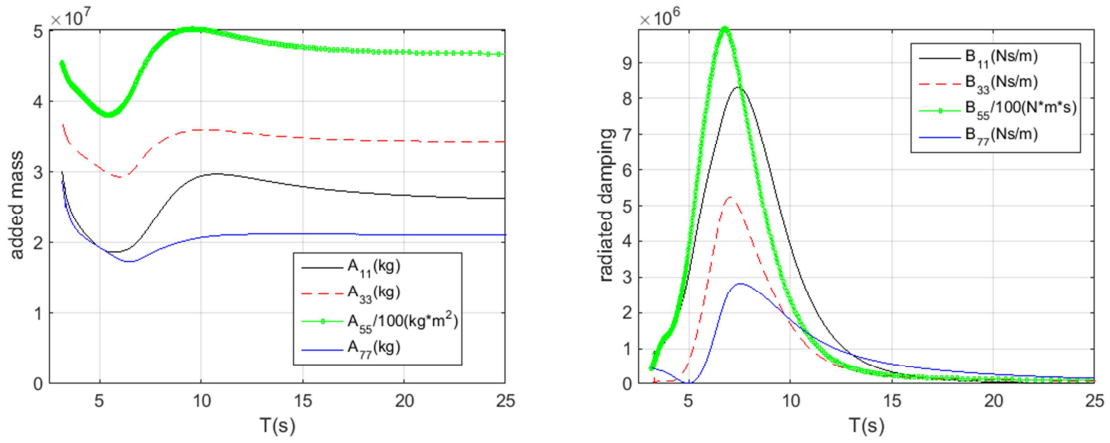

(a) Self-radiated added mass/moment of inertia (b) Self-radiated damping coefficients

Figure 5 Added mass for different motion modes (note: added moment of inertia and radiated damping coefficient for pitch have been divided by 100 for better comparisons)

3.4.2 Cross-radiated added mass and damping coefficients

Cross-radiated added masses from other motion modes on surge motion have shown that only the heave motions of both structure & piston and the pitch motion would have significant effects since these cross-terms (added masses and damping coefficients) have comparable magnitudes (positive or negative) to the self-radiated terms (see Figure 6a and Figure 7a), while the sway, roll and yaw motions have little effects on the cross-terms to surge (Figure 6b and Figure 7b). Obviously, these motions (surge, heaves and pitch) are strongly coupled each other.

It is also seen that the coupling effects can be either positive or negative manner. From the mathematical equation, the positive and negative cross-term added masses can be understood as following: a positive A_{13} means that an increased heave motion (structure) will cause a decrease in surge motion, and negative A_{15} and A_{17} mean that the increased pitch motion (pitching nose down is positive) and heave motion of the piston will induce an increase in the surge motion.

Similarly, for the structure heave motion, see Figure 6c and Figure 7c, large coupling effects could come from surge, pitch and piston heave. From Figure 6d and Figure 7d, it can be seen that the pitch motion is strongly coupled with the piston heave motion.

In all, for the RM6 BBDB device, the surge, heave (structure), pitch and the piston heave are all strongly coupled, while other motion modes (sway, roll and yaw) are not coupled to these motions. From the point of view of wave energy conversion, only surge, heave, pitch (structure) and the heave (piston) will contribute.

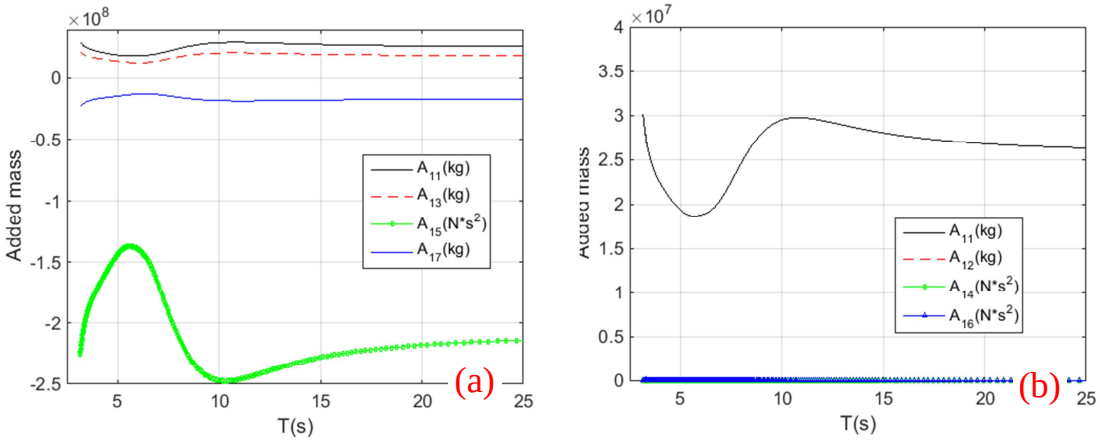

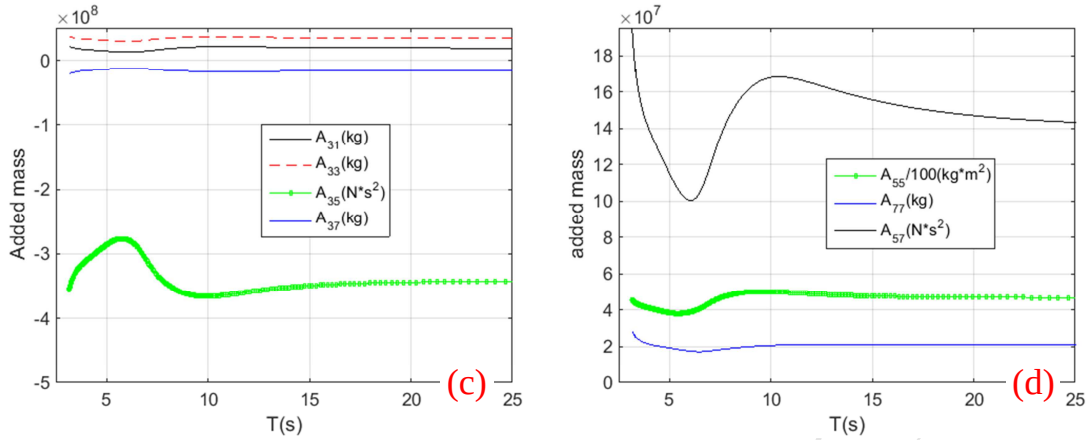

Figure 6 Cross-radiated added mass/moment of inertia

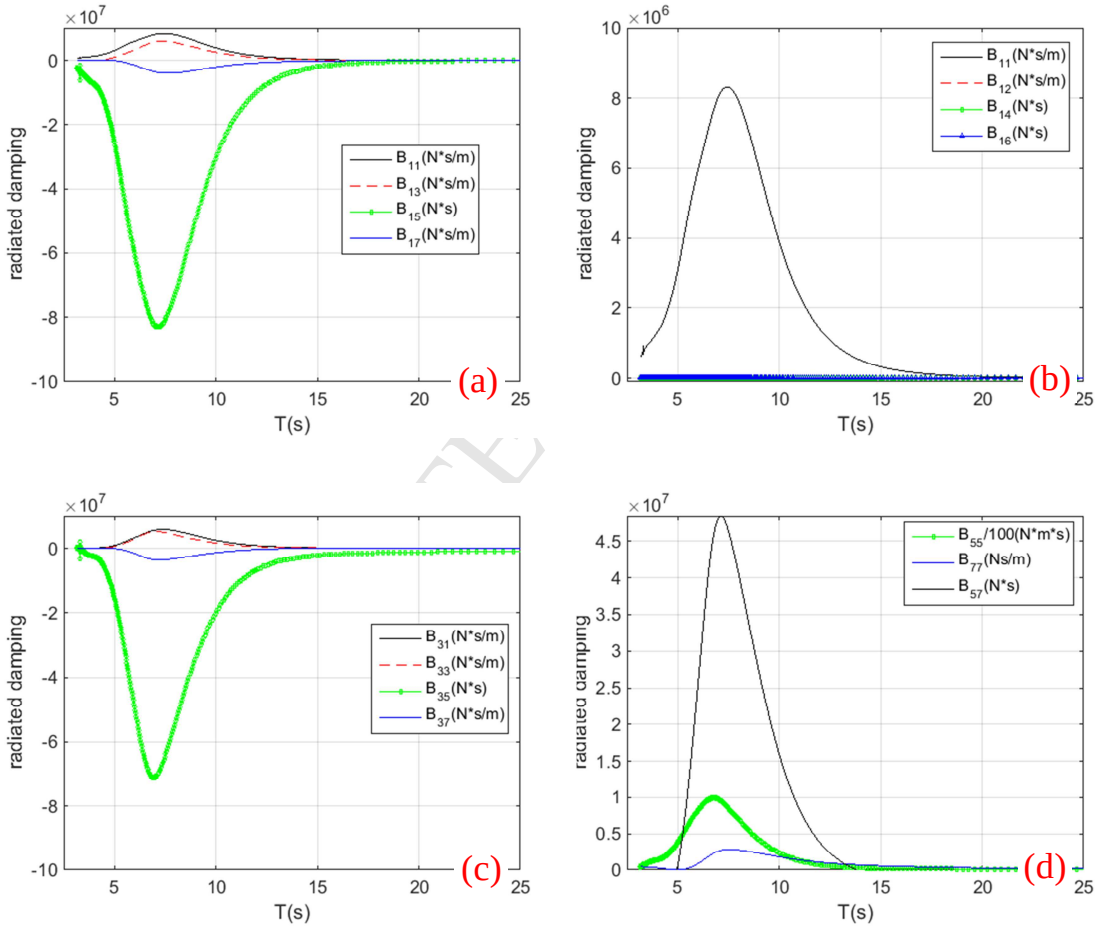

Figure 7 Cross-radiated damping coefficients

3.5 Decoupled motions

In the numerical modelling, it is possible to study the fully decoupled motions of the structure and the piston. This can be done by setting all the cross terms as zeros in the dynamic equation (3), that is,

$$\begin{pmatrix} a_{11} & 0 & 0 & 0 & 0 & 0 & 0 \\ 0 & a_{22} & 0 & 0 & 0 & 0 & 0 \\ 0 & 0 & a_{33} & 0 & 0 & 0 & 0 \\ 0 & 0 & 0 & a_{44} & 0 & 0 & 0 \\ 0 & 0 & 0 & 0 & a_{55} & 0 & 0 \\ 0 & 0 & 0 & 0 & 0 & a_{66} & 0 \\ 0 & 0 & 0 & 0 & 0 & 0 & a_{77} \end{pmatrix} \begin{pmatrix} X_1 \\ X_2 \\ X_3 \\ X_4 \\ X_5 \\ X_6 \\ X_7 \end{pmatrix} = \begin{pmatrix} F_1 \\ F_2 \\ F_3 \\ F_4 \\ F_5 \\ F_6 \\ F_7 \end{pmatrix} \quad (6)$$

Principally, the fully de-coupled dynamics can hardly be fully reproduced in physical modelling, because in physical modelling, it is possible to limit certain motions. For instance, a mechanism can be used to allow only heave motion of the structure (identified as 'heave only (structure)') while other motion modes are limited. However, for the BBDB OWC device, the heave motion of the water body in the water column is always present regardless of the structure motion modes, even for the fixed structure. As such, the heave motions of the structure and of the piston will still couple together in reality. One special decoupled case in physical modelling is the fixed OWC, in which only the heave motion of the piston is allowed, thus it is fully decoupled from all the motion modes of the structure.

In numerical modelling of the decoupled motion analysis, it is easy to fully decouple all the motions, and it provides a good way to examine the natural resonance periods for all motion modes, while they may be impossible to obtain from physical modelling. Solving Eq. (6) yields the decoupled resonance periods as in the following table.

Table 2 Motion natural periods using the decoupled method

Motion mode	Resonance period (s)	description
Surge	~73.92s	K_1=200,000 N/m
Sway	~75.00s	K_2=200,000 N/m
Heave	18.76s	Decoupled
Roll	18.76s	Decoupled
Pitch	15.14s	Decoupled
Yaw	~250s	K_6=2,000,000 Nm
Piston	13.75s	Fix OWC/decoupled

The RAOs for the fully decoupled motions are plotted in *Figure 8*, and it can be seen that these are the typical RAOs for the independent motions, with a large peak at the resonance periods. However, if all these decoupled RAOs are plotted against the IWS RAO in motion coupling, an interesting comparison can be seen in Figure 9: 3 peaks in the IWS RAO are corresponding to 3 different periods, i.e., 8.61s, 12.08s and 16.11s, while are all different from the resonance periods of structure heave (18.76s), pitch (15.14s) and the piston heave (13.75). Due to the strong coupling between different motion modes, the individual resonances will no longer present directly in the IWS RAO, with its peaks being different from the main contributors: the heave (structure), pitch and heave (piston). This is essentially very different from the symmetrical OWC as studied in [28]: for an axi-symmetrical spar OWC, its two peaks in IWS RAO are directly linked to the resonance of the structure heave and the piston heave motions (they are only weakly coupled).

Because the strong couplings among the motion modes, especially the surge, heave and pitch (structure) and the heave (piston), to get an expected response for the IWS motions (which can be regarded as a good indicator for power performance since a high RAO in IWS means a possible high power conversion capacity), the optimisation of the BBDB OWC wave energy converter needs a systematic approach, rather than a simple adjustment of one individual resonance periods. In this research (including the second part), a systematic approach will be carried out to optimise the device design so a better hydrodynamic and thus power performance may be achieved using the optimisation approaches.

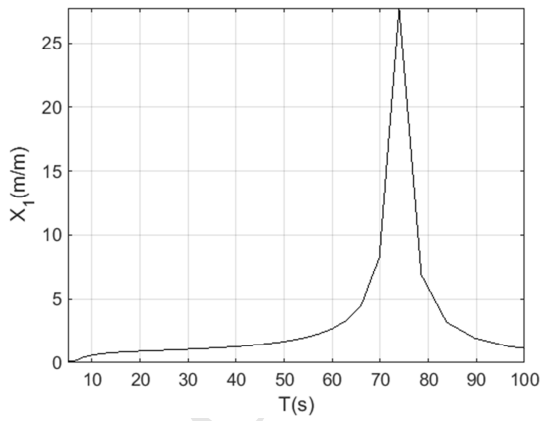

(a) Surge RAO: ~73.92s

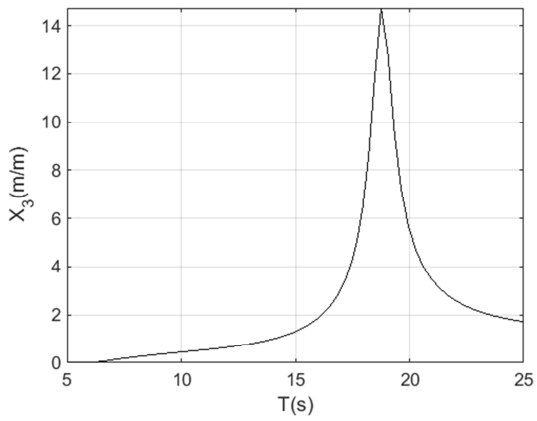

(b) Heave RAO (structure): 18.76s

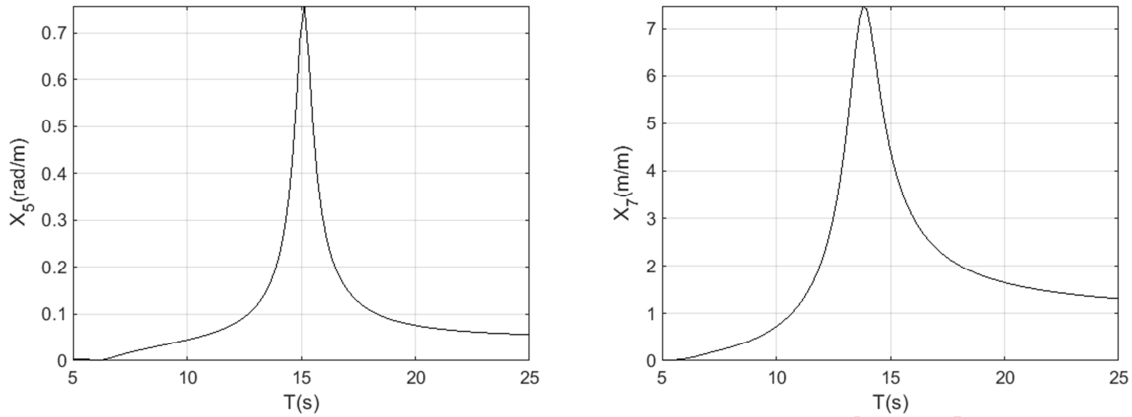

(c) Pitch RAO: 15.14s (d) Heave RAO (piston): 13.75s

Figure 8 RAOs of the decoupled motions in waves (with the linear viscous damping)

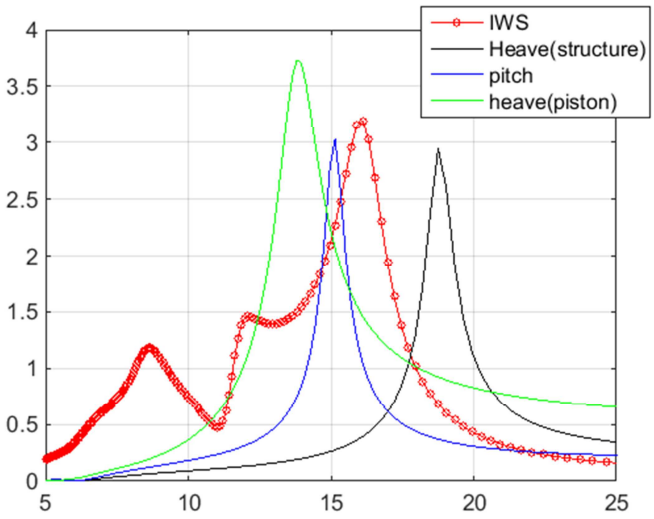

*Figure 9 IWS RAO against decoupled RAOs of the relevant motion modes (all with viscosity). Note: the decoupled RAOs have been scaled for comparison: heave (structure)*0.2; pitch*4; heave (piston)*0.5*

4 VALIDATION

To validate the numerical method schemed in the previous sections, the responses of the water body motion and the IWS motion from the numerical modelling are compared to the experimental data (the experimental data are taken from Ref. [23]). Figure 10 and Figure 11 give the comparisons of the water body (piston) motion and the IWS motion, i.e., the relative heave motion between the water body and the structure, respectively. The numerical modelling results agree quite well with the experimental data. From the comparisons, it can be seen that the main features of the RAOs of the piston heave motion and the internal water surface (IWS) motion are both well predicted, though the peak values may not be well

predicted in the numerical modelling. Considering the general linear viscous damping coefficients using Eq. (5), the RAOs of the piston heave motion and the IWS motion are both slightly over damped. But as a generic formulation, Eq. (5) is still considered to be a good generic expression.

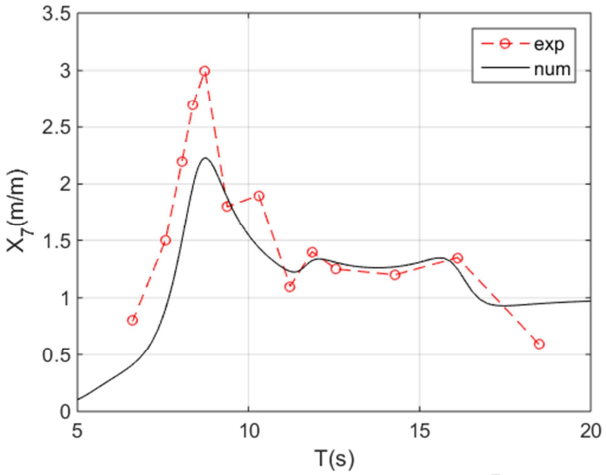

Figure 10 Water body motion RAOs (comparison of numerical modelling and physical model test data)

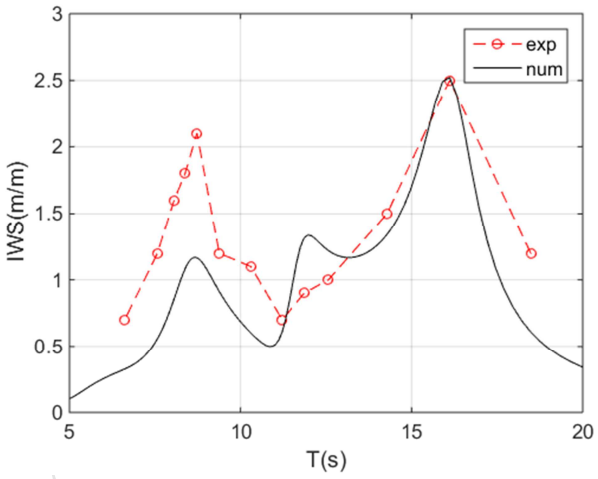

Figure 11 IWS motions in the BBDB RM6 wave energy converter

5 MOTION COMPARISONS AND OPTIMISATIONS

In this section, motion RAO comparisons will be made for different scenarios, including different device orientations, duct lengths, water column sizes and mooring stiffness. The comparisons will be made for the motions of structure surge, heave and pitch and of the piston heave, with special attention to the motion of the internal water surface (IWS), which is the most important factor for wave energy

conversion for the BBDB OWC devices (more details can be found in the second part of the research [38]).

5.1 BBDB and FBDB

An interesting factor is the orientation of the bent duct buoy. From all the experience and the relevant research work, the backward bent duct buoy (i.e., 'BBDB') is proposed because this is the orientation the bent-duct OWC device is most efficient (see the wave direction for BBDB in *Figure 2*). Here a comparison is made to the forward bent duct buoy ('FBDB'), for which the wave comes to the duct opening, i.e, the BBDB and FBDB are orientated in waves in 180° difference. Figure 12 shows the comparisons for different motion modes. For the heave motions of the structure, small heave RAOs can be seen for the waves with periods of 5-15s for FBDB (Figure 12a). For the pitch motions, again small difference in RAOs can be seen at both small and large wave periods, while there is no significant difference for wave periods between 10s and 15s (Figure 12b). For the heave motion of the piston, large deficits in RAO happen in the wave periods of 5s to 10s for FBDB, especially the piston heave RAO for FBDB is very small at the wave periods from 5-7.5s. When the wave period is larger than 10s, these two orientations have very close RAOs.

Under the strong coupling of above motions, the IWS motions shows a complicated combination (Figure 12d). The BBDB IWS RAO is larger than the FBDB IWS RAO, except the wave periods between 10s and 12s for which the FBDB IWS RAO is slightly larger than that of BBDB. The largest difference in the RAOs is in the wave periods below 8s, where the FBDB has very small IWS RAOs, which could be a worst IWS RAO in terms of wave energy conversion (details can be seen in the second part of the research).

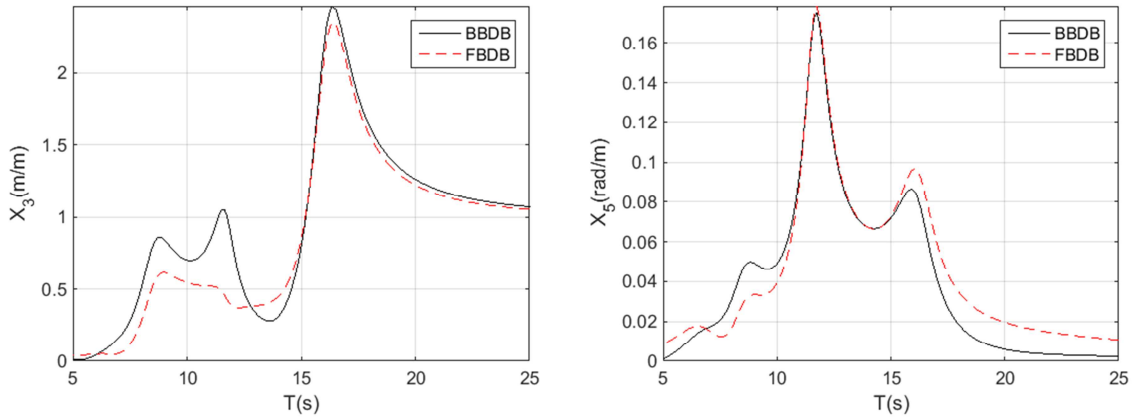

(a) Heave RAOs (structure) (b) Pitch RAOs

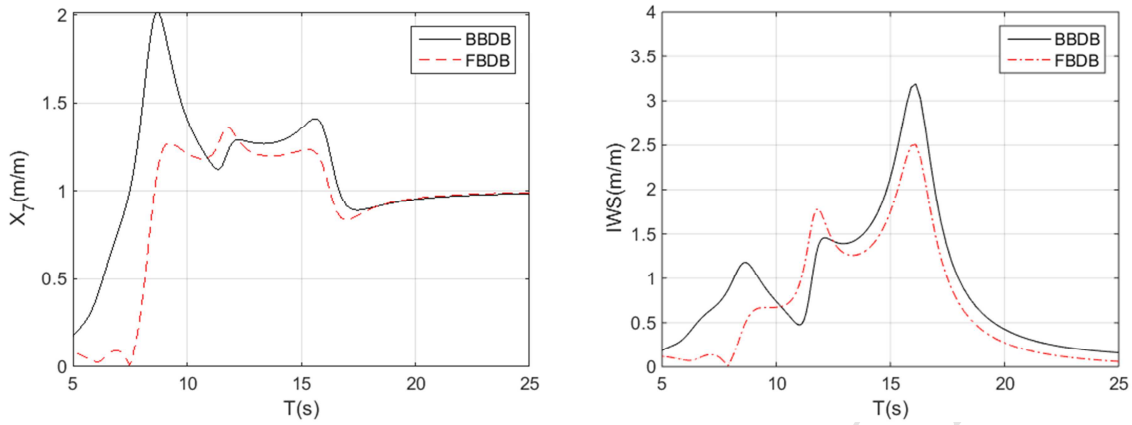

(c) Heave RAO (piston) (d) IWS RAO

Figure 12 RAO comparison for BBDB and FBDB

5.2 Effect of wave angles

It is well known that the BBDB OWC device has a highest energy conversion efficiency when the incoming waves head to the back of the BBDB device. Hence, the BBDB devices are generally deployed heading to the dominant wave direction at the site. However, in reality, waves may propagate to the device in different directions. Following example is a comparison of the motions of the device in head waves and in 45° waves. For the heave motion of the structure, large difference can be seen near the peaks and troughs (Figure 13a) while relatively smaller difference can be found in the heave motion of the piston (Figure 13c). For the pitch motion (Figure 13b), some difference can be seen, with the pitch RAO for FBDB having smaller magnitude.

From Figure 13d, it can be seen that the IWS RAO in 45° waves is smaller than that in the head waves, which is an indicator that the device is less efficient in 45° waves than in head waves.

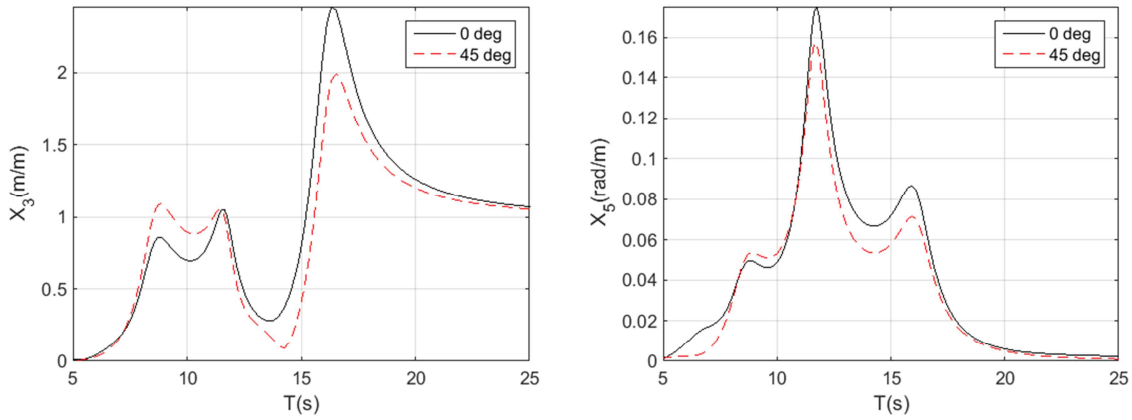

(a) Heave RAOs (structure) (b) Pitch RAOs

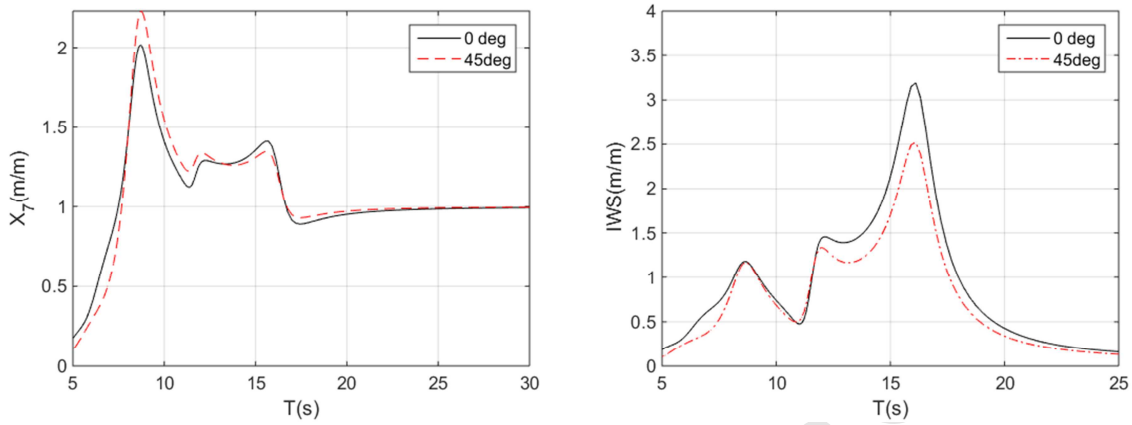

(c) Heave RAO (piston) (d) IWS RAO

Figure 13 RAO comparisons in head wave and in waves of 45°

5.3 Cases with limited motions

In the section, attention is paid to the cases of limited/isolated motions, the cases that the structure motions are limited to the given motion mode. For instance, 'surge only' means the device structure can only move in surge whilst all other motion modes (structure) are set to zeros. The same methods are applied for heave and pitch only, in which the structure heave and pitch are only allowed. A very special case is the case with a fixed structure ('fix'), which means the device structure is fixed, hence no structure motions are allowed.

It must be noted that such isolated motion scenarios, the water body in the water column will not be limited, hence the heave motion of the piston is allowed in all the isolated cases. Also, it will be seen in the flowing comparisons that the heave motion of the piston is always strongly coupled with the given motion mode of the structure.

All comparisons are made for the allowed motions against the decoupled motions (from Eq. (6)). As a decoupled motion in mathematics, it is fully isolated from effect or coupling from other motion modes. Figure 14 shows the comparisons of the isolated motion and the decoupled motion. Due to the coupling of the isolated motions with the water body in the water column, the heave and pitch motions in their motion-isolated cases are very different from the decoupled motions, with RAO peaks happening at different wave periods (see Figure 14b and Figure 14c) while the surge motion has different in the peak in the RAOs, and there is a small peak in the surge only for the wave at period of 10s (Figure 14a), which is actually caused by the coupling of the surge and the water body in the water column.

In the fixed case, the water body motion is fully isolated from any other motion modes of the structure physically, hence it is exactly as in same condition as the decoupled case for the heave motion of the piston. As a result of this, these two RAOs are identical (Figure 14d).

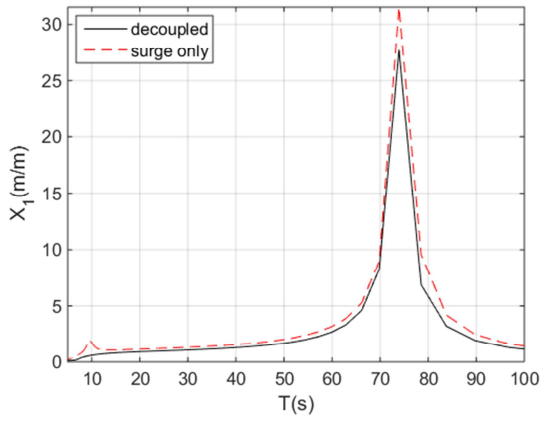

(a) Decoupled surge and surge only

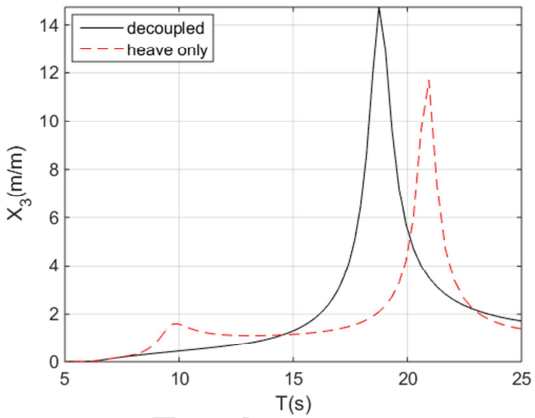

(b) Decoupled heave and heave (structure) only

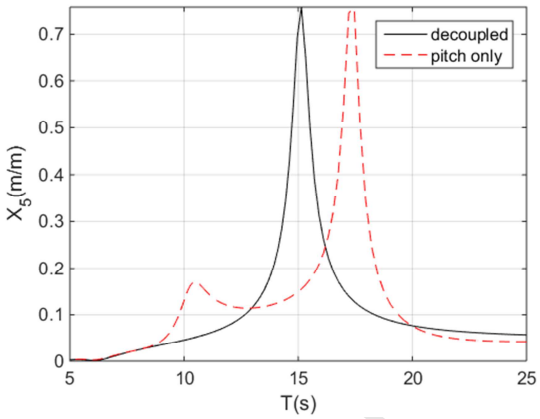

(c) Decoupled pitch and pitch only

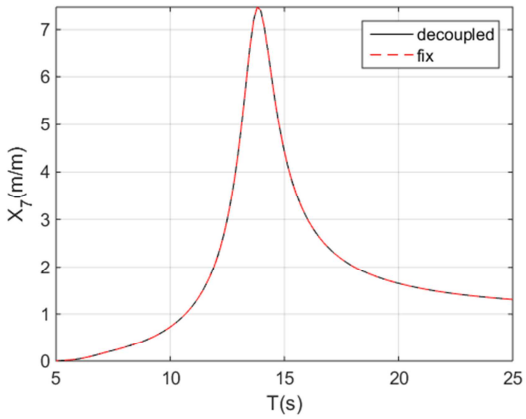

(d) Decoupled heave (piston) and fix device

Figure 14 RAO comparisons of the decoupled and isolated motions

5.4 Effect of horizontal duct lengths

Duct length of the BBDB devices have large effects on the motions of the device (and eventually to the energy conversion efficiency). The following case is the comparison of the motion RAOs for the devices with different duct lengths. For a fair and simple comparison, all the device parameters (such as the centre of gravity, the displacement, the moment of inertia) are kept unchanged and achievable. Hence the differences are mostly caused due to the added mass and damping coefficients as well as the excitation forces on the structure and the water body in the water column.

Figure 15 shows the comparisons of the motion RAOs for two different duct lengths. The original design is same as the RM6 [23, 28], which has an overall duct length of 35m, and a longer duct ('10m longer') means the duct length is 10m longer, i.e, the overall duct length is 45m. Due to the change in duct length, the motion RAOs are changed. For the heave RAO (structure), two peaks can be seen, rather than 3 peaks in the original design, with peaks happening at a slightly larger wave periods (Figure 15a). Obviously, the largest difference is seen for the pitch motions (Figure 15b). The RAO change in pitch is dramatic, in which 3 peaks are more evenly distributed, including the peak values, whilst in the original design, the pitch has a dominant response in the wave period of 12s.

The heave motion (piston) has changed, similarly to the heave motion of the structure. Again, the peaks can be seen happening at the slightly larger wave periods for the longer duct (Figure 15c).

An interesting result can be seen of the IWS motions (Figure 15d). With a longer duct, the RAO is smoother than the original design. Unlike the original design, where there is a deficit at the wave period of 11s (this is very unfavourable for wave energy conversion, see [28]), the device with a longer duct does not have such a deficit, hence it is beneficial for improving wave energy conversion.

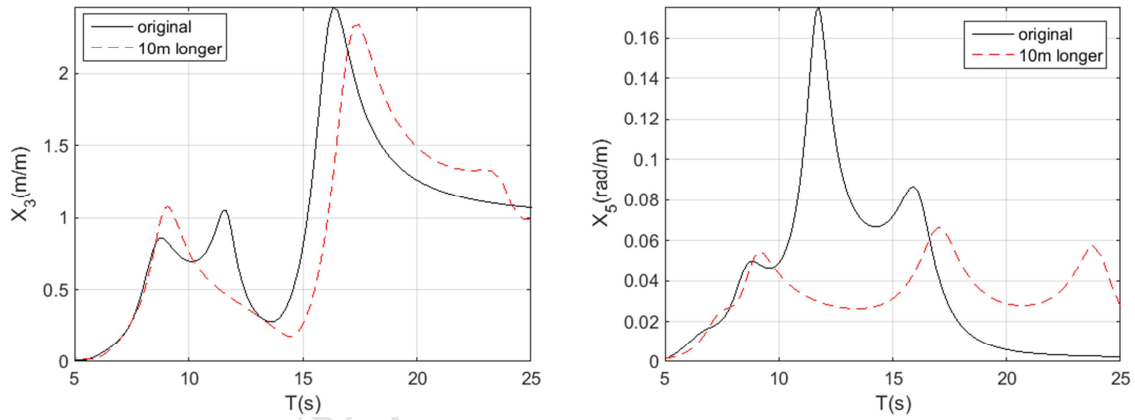

(a) Heave RAOs (structure) (b) Pitch RAOs

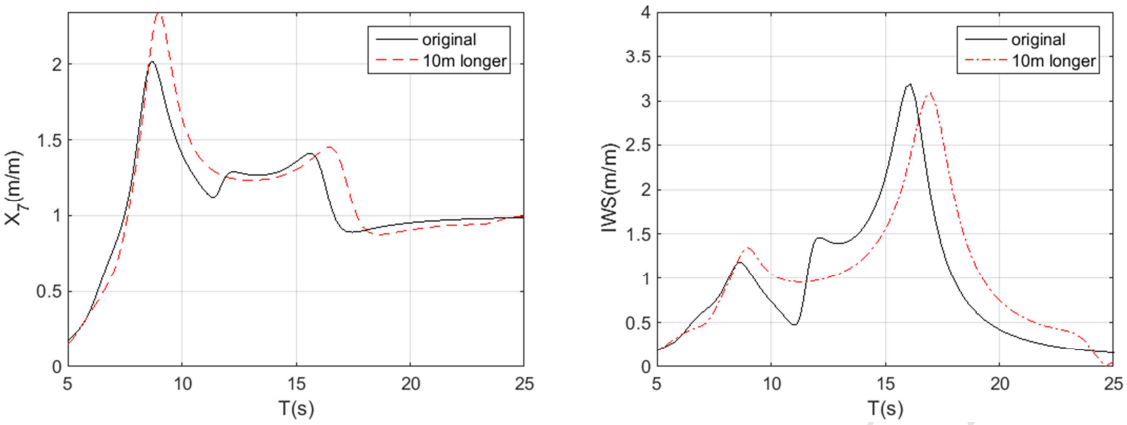

(c) Heave RAO (piston) (d) IWS RAO

Figure 15 RAO comparisons of the original BBDB and longer BBDB

5.5 Effect of mooring stiffness

An interesting finding in the numerical modelling is the effect of the mooring stiffness on the motions. Conventionally, mooring system is designed to confine the device within a pre-defined profile and hence the device can only move with a limited excursion, even in the extreme wave conditions. For such a purpose, the conventional mooring may have a relatively small stiffness, thus its resonance periods for surge, sway and yaw motions are quite large (normally more than 60s, and in this case, about 74s) to avoid the resonance in the energetic waves. However, as a case study here, the mooring stiffness is increased 10 times (from 200 kN/m to 2000 kN/m), the surge resonance period is changed from 74s to 29s (Figure 16a). Since the coupling among the surge motion to other motion modes, the heave motions (structure and piston both) and pitch motion are all affected (Figure 16b-d), with a significant change on pitch motion (Figure 16c) even at small wave periods. When a larger mooring stiffness is applied, the IWS RAO has changed accordingly (Figure 16e). With a stiffer mooring, it is possible to improve the motion performance for the wave periods less than 15s, for which most interested waves are included for wave energy conversion. Hence it is possible to improve the BBDB device power performance using a stiffer mooring.

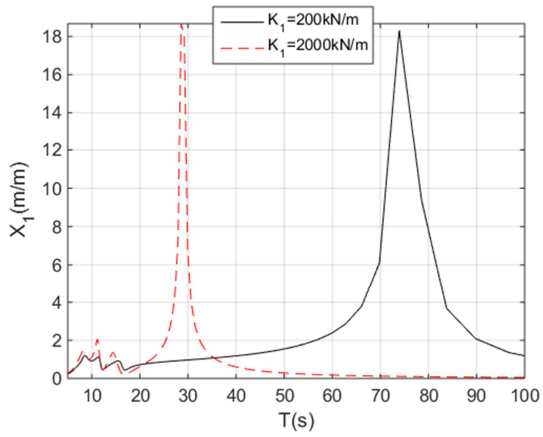

447

448 (a) Surge RAOs

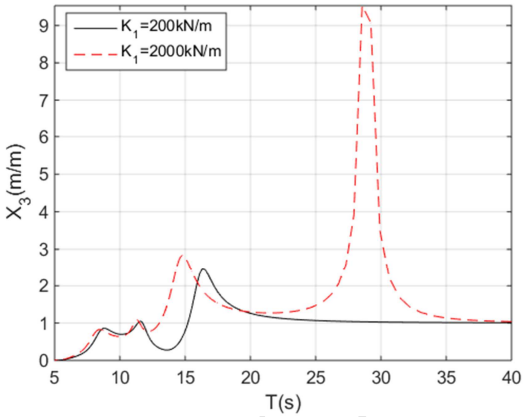

(b) heave RAOs (structure)

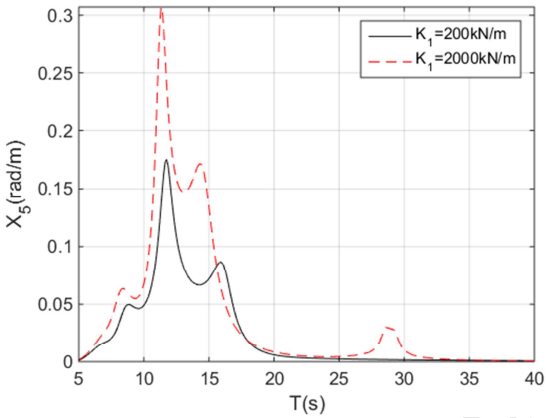

449

450 (c) pitch RAOs

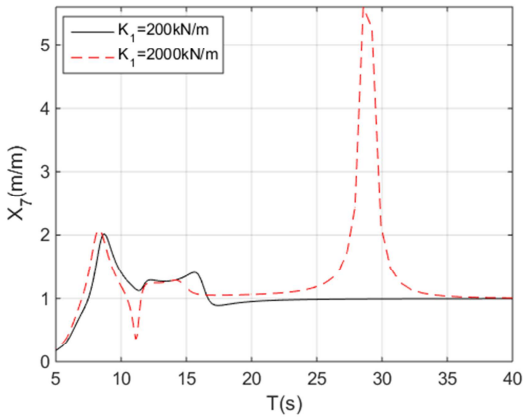

(d) heave RAOs (piston)

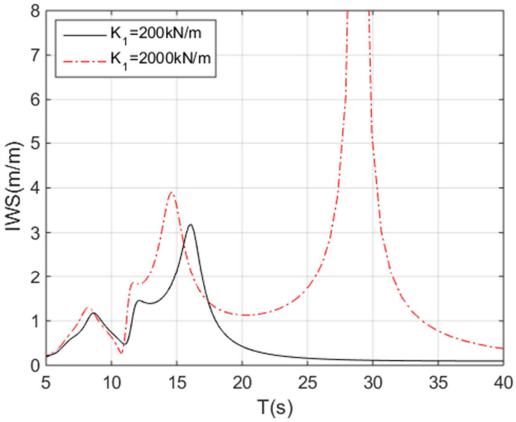

451

452 (e) IWS RAOs

453 *Figure 16 RAO comparisons of the different mooring stiffness*

5.6 Modification of vertical water column

In the original design of RM6, the vertical water column has a larger area (17.5m×27m) than that of the horizontal column (14m×27m). In a modification of the design, a study is made to the modified vertical column size, so the vertical water column has a same size as that of horizontal water column (14m×27m, 'new water column'). The motion comparisons are seen in Figure 17. As a simple purpose for the uniform water column, it is to avoid the fluid being accelerated or decelerated when the flow move in the different size of the water column. However, the hydrodynamic changes are much more than the accelerated or decelerated flow. Due to the change of the vertical water column, significant changes can be seen in the structure heave and pitch RAOs (Figure 17a & b). Relatively, the change for the piston heave RAO is less dramatic, however, a much enlarged peak can be seen at the wave period of about 8s (Figure 17c).

As a result of the change, the IWS RAO shows very a good increase for the wave period less than 15s, and the largest benefit would be the removal of the deficit in the IWS RAO as shown in the original design (Figure 17d), though the modification may lead to less efficient for longer wave (more than 15s). Since we are not very interested in long waves (its occurrence is low), it can be expected that the changed water column may be very beneficial for improving wave energy extraction from seas.

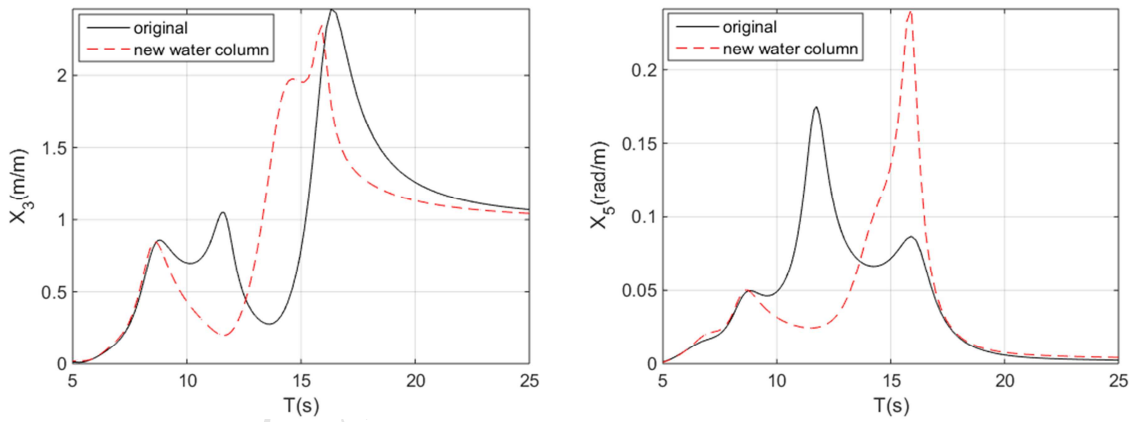

(a) Heave RAOs (structure) (b) Pitch RAOs

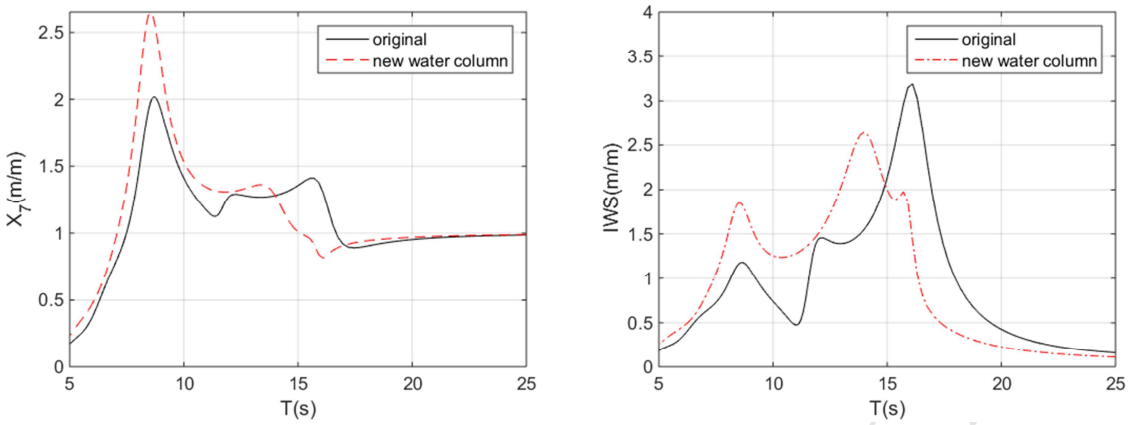

(c) Heave RAO (piston) (d) IWS RAO

Figure 17 RAO comparisons of the original water column and the new water column (uniform)

6 CONCLUSIONS

The backward bent duct buoy (BBDB) oscillating water column wave energy converters are very promising wave energy converters because of their unique features using multiple motion modes to enhance its power performance. This research provides the methods for hydrodynamic analysis and thus for optimising the BBDB OWC wave energy converters so for maximising wave energy conversion for the BBDB OWC wave energy converters. From the study, following conclusions can be drawn:

- Due to the non-symmetry of the BBDB OWC devices, the motions of the structure surge, heave and pitch and of the 'piston' heave are all strongly coupled, and these motions must be solved in a coupled manner so for studying the hydrodynamic performance (the energy conversion as well) of the BBDB devices.
- The internal water surface (IWS) motions is essentially a result of the strong couplings among these motions. Individual resonance periods from the de-coupled model can be very different from those shown in the coupled responses. Hence a change of one individual resonance period may induce some complicated results. As such, the optimisations must be carried out in a systematic manner.
- It has been shown that the backward bent duct would have much better hydrodynamic performance (thus the power performance) than the forward bent duct in terms of hydrodynamic performance in the wave periods of 5-10s (which cover the main waves for wave energy conversion). When waves come from a different direction (for instance 45°), a reduction of the hydrodynamic performance (mainly on IWS response) would be expected.

- Longer horizontal duct could significantly improve the hydrodynamic performance in terms of wave energy conversion in the case of RM6 design.
- Using a uniform size of the water column may improve the hydrodynamic response, especially the removal of the deficit in the IWS response (around 11s). This can be regarded as an indicator of a better power performance for the device.
- Mooring system could be an effective factor for improving wave energy conversion, since it is possible to use a stiffer mooring to increase the hydrodynamic performance of the BBDB device for the purpose of wave energy conversion.

ACKNOWLEDGEMENTS

The author would like to thank the friends and the former colleagues and friends for their help when I was with MaREI, University College Cork, Ireland.

REFERENCES

1. EC, *Study on lessons for ocean energy development*, 2016, cited at: http://publications.europa.eu/resource/cellar/3a4f6411-6777-11e7-b2f2-01aa75ed71a1.0001.01/DOC_1
2. Magagna, D., R. Monfardini, and A. Uihleih, *JRC Ocean Energy Status Report 2016 Edition: Technology, market and economic aspects of ocean energy in Europe*, 2016, cited at: https://setis.ec.europa.eu/sites/default/files/reports/ocean_energy_report_2016.pdf (11/12/2017)
3. Falcao, A., 2010. Wave energy utilization: a review of the technologies. *Renewable and Sustainable Energy Reviews*, **14**(3): pp. 899-918. doi: 10.1016/j.rser.2009.11.003.
4. Masuda, Y., et al. 1988, The backward bend duct buoy-an improved floating type wave power device. *Proceedings of OCEANS '88. A Partnership of Marine Interests*. 31 Oct-2 Nov. 1988. Baltimore, USA.
5. Ross, D., *Power from sea waves*. 1995: Oxford University Press.
6. Evans, D.V., 1978. The oscillating water column wave-energy device. *IMA Journal of Applied Mathematics*, **22**(4): pp. 423-433. doi: 10.1093/imamat/22.4.423.
7. Masuda, Y. 1979, Experimental full-scale results of wave power machine Kaimei in 1978. *Proceedings of the 1st Symposium on Wave Energy Utilization,*. 30 Otc.-1st Nov. 1979. Gothenburg, Sweden.
8. Evans, D.V. and R. Porter, 1995. Hydrodynamic characteristics of an oscillating water column device. *Applied Ocean Research*, **17**(3): pp. 155-164. doi: 10.1016/0141-1187(95)00008-9.
9. Sheng, W. and A. Lewis, 2016. Wave energy conversion of oscillating water column devices including air compressibility. *Journal of Renewable and Sustainable Energy*, **8**: pp. 054501. doi: 10.1063/1.4963237.
10. O'Sullivan, D.L. and A. Lewis, 2010. Generator selection and comparative performance in offshore oscillating water column ocean wave energy converters. *IEEE Transactions on Energy Conversion*, **26**(2): pp. 603-614. doi: 10.1109/TEC.2010.2093527.
11. Folley, M., R. Curran, and T. Whittaker, 2006. Comparison of LIMPET contra-rotating wells turbine with theoretical and model test predictions. *Ocean Engineering*, **33**(8-9): pp. 1056-1069. doi: 10.1016/j.oceaneng.2005.08.001.
12. Boake, C., T. Whittaker, and M. Folley. 2002, Overview and initial operational experience of the LIMPET wave energy plant. *Proceedings of The Twelfth (2002) International Offshore and Polar Engineering Conference*. May 26–31, 2002. Kitakyushu, Japan.
13. Le Crom, I., et al. 2009, Numerical Estimation of Incident Wave Parameters Based on the Air Pressure Measurements in Pico OWC Plant *Proceedings of the 8th European Wave and Tidal Energy Conference*. 7-10 Sep. 2009. Uppsala, Sweden.
14. Neumann, F. and I. Le Crom. 2011, Pico OWC - the Frog Prince of Wave Energy? Recent autonomous operational experience and plans for an open real-sea test centre in semi-controlled environment. *Proceedings of the 9th European Wave and Tidal Energy Conference*. 5-9 Sep. 2011. Southamplton, UK.

15. Henriques, J.C.C., et al. 2017, A comparison of biradial and Wells air turbines on the Mutriku breakwater OWC wave power plant. *Proceedings of the ASME 2017 36th International Conference on Ocean, Offshore and Arctic Engineering*. June 25-30, 2017,. Trondheim, Norway.
16. Torre-Enciso, Y., et al. 2009, Mutriku Wave Power Plant: from the thinking out to the reality. *Proceedings of the 8th European Wave and Tidal Energy Conference*. 7-10th Sep. 2009. Uppsala, Sweden.
17. Alcorn, R., M. Healy, and A.W. Lewis. 2012, Lessons learned from the Galway bay Seatrials of the EU funded CORES project. *Proceedings of the 4 International Conference on Ocean Energy*. 17-19 Oct. 2012. Dublin, Ireland.
18. OceanEnergy, *Ocean Energy: A World of Power*, 2015, cited at: http://www.oceanenergy.ie/ (15/10/2017)
19. Heath, T., 2012. A review of oscillating water columns. *Philosophical Transactions of the Royal Society A: Mathematical, Physical & Engineering Sciences*, **370**: pp. 235-245. doi: 10.1098/rsta.2011.0164.
20. Mavrakos, S.A. and D.N. Konispoliatis. 2012, Hydrodynamic analysis of a vertical axisymmetric oscillating water column device floating in finite depth waters. *Proceedings of the ASME 31st International Conference on Ocean, Offshore and Arctic Engineering*. July 1-6, 2012. Rio de Janeiro, Brazil.
21. Evans, D.V., 1982. Wave-power absorption by systems of oscillating surface pressure distributions. *Journal of Fluid Mechanics*, **114**: pp. 481-499. doi: 10.1017/S0022112082000263.
22. Babarit, A., et al., 2011, Numerical estimation of energy delivery from a selection ofwave energy converters, Final Report, Ecole Centrale de Nantes & Norges Teknisk-Naturvitenskapelige Universitet. Cited at:
23. Bull, D., et al., 2014, reference Model 6 (RM6): Oscillating wave energy converter, SANDIA2014-18311, Sandia National Laboratory. Cited at:
24. Lopez, I., et al., 2016. Holistic performance analysis and turbine-induced damping for an OWC wave energy converter. *Renewable Energy*, **85**: pp. 1155-1163. doi: 10.1016/j.renene.2015.07.075.
25. Lee, C.H. and F.G. Nielsen. 1996, Analysis of oscillating-water-column device using a panel method. *International Workshop on Water Wave and Floating Bodies*. 17-20, Mar. 1996. Hamburg, Germany.
26. Falcao, A., J.C.C. Henriques, and J.J. Candido, 2012. Dynamic and optimization of the OWC spar buoy wave energy converter. *Renewable Energy*, **48**: pp. 369-381. doi: 10.1016/j.renene.2012.05.009.
27. Sheng, W., R. Alcorn, and A.W. Lewis, 2014. Assessment of primary wave energy conversions of oscillating water columns. II. Power take-off and validations. *Journal of Renewable and Sustainable Energy*, **6**: pp. 053114. doi: 10.1063/1.4896851.
28. Bull, D., 2015. An improved understanding of the natural resonances of moonpools contained within floating rigid-bodies: Theory and application to oscillating water column devices. *Ocean Engineering*, **108**: pp. 799-812. doi: 10.1016/j.oceaneng.2015.07.007.
29. Kurniawan, A., J. Hals, and T. Moan. 2011, Modelling and simulation of a floating oscillating water column. *Proceedings of the ASME 2011 30th International Conference on Ocean, Offshore and Arctic Engineering*. June 19-24, 2011. Rotterdam, The Netherlands.
30. Falnes, J., *Ocean Waves and Oscillating Systems: Linear Interaction Including Wave-Energy Extraction*. 2002: Cambridge University Press.
31. Nagata, S., et al. 2011, Frequency domain analysis on primary conversion efficiency of a floating OWC-type wave energy converter 'Backward bent Duct Buoy'. *Proceedings of the 9th European Wave and Tidal Energy Conference*. 5-9 Sep, 2011. Southampton, UK.
32. Lewis, A., T. Gilbaud, and B. Holmes. 2003, Modelling the Backward Bent Duct Device-B2D2, a comparison between physical and numerical models. *Proceedings of 5th European Wave Energy Conference*. 17-20th, Sep. 2003. Cork, Ireland.
33. Hong, D.C., S.Y. Hong, and S.W. Hong, 2004. Numerical study on the reverse drift force of floating BBDB wave energy absorbers. *Ocean Engineering*, **31**(10): pp. 1257-1294. doi: 10.1016/j.oceaneng.2003.12.007.
34. SNL, *Reference Model Project (RMP)*, 2017, cited at: http://energy.sandia.gov/energy/renewable-energy/water-power/technology-development/reference-model-project-rmp/ (10/02/2018)
35. Neary, V.S., et al., 2014, Methodology for Design and Economic Analysis of Marine Energy Conversion (MEC) Technologies, SAND2014-9040, Sandia National Laboratories, USA. Cited at:
36. WAMIT, *User Manual*, 2016, cited at: http://www.wamit.com/manual.htm (20/01/2016)
37. Newman, J.N., *Marine Hydrodynamics*. 1977: The MIT Press, Cambridge, Massachusetts, USA.
38. Sheng, W., 2018. Motion and performance of BBDB OWC wave energy converters: II, Power conversion. *Prepared for journal publication.*

Highlights:

- Formulate the Hydrodynamic equation for BBDB oscillating water column wave energy converters.
- Provide the decoupled hydrodynamic model for further understanding of the coupling between motions.
- Perform the analyses of hydrodynamic performance of the BBDB device.
- Optimise the BBDB device for better hydrodynamic performance.